WORLD JOURNAL OF PHARMACEUTICAL RESEARCH
SJIF Impact Factor 8.074
Volume 7, Issue 7, 160-191. Research Article ISSN 2277– 7105

CHARACTERIZATION OF A NOVEL TAYLOR-COUETTE ULTRAVIOLET REACTOR FOR NON-THERMAL PASTEURIZATION OF MILK

Rawa Abdul Redha Aziz[1]* and Keith Warriner[2]

[1]Department of Microbiology, College of Science, Al-Karkh University for Science, Baghdad. Iraq.

[2]Department of Food Science, OAC, University of Guelph, Ontario, Canada.

Article Received on
13 Feb. 2018,

Revised on 05 March 2018,
Accepted on 26 March 2018,

DOI: 10.20959/wjpr20187-11762

***Corresponding Author**
Dr. Rawa Abdul Redha Aziz
Department of Microbiology, College of Science, Al-Karkh University for Science, Baghdad. Iraq.

ABSTRACT

Disinfection of milk by a novel UV reactor based on Taylor-Couette vortex flow has been evaluated as part of an effort to develop non-thermal processing technology for pasteurizing milk. By using *Bacillus subtilis* endospores and bacteriophages as model microbes, it was demonstrated that level of inactivation was dependent on the flow-pattern of the milk passing through the reactor. The highest level of microbial inactivation was achieved at the transition from laminar wavy vortices (WV) to laminar modulated wavy vortices (MWV). The stability of the generated Taylor-Couette vortices could be enhanced when increasing the viscosity of the milk although this did not translate to higher levels of microbial UV inactivation. Tryptophan and cysteine provided protection to the microbes by absorbing UV photons. Although the actual UV dose required to inactive *Escherichia coli* in milk was comparable to the efficacy of other reactors, only a 1 log cfu reduction in numbers could be achieved under optimal operating conditions. The poor stability of generated vortices coupled with UV absorption effects of milk constituents would limit the application of the reactor for non-thermal pasteurization of opaque fluids.

KEYWORDS: Ultraviolet, Taylor-Couette reactor, MWV, pasteurization**.**

INTRODUCTION

Raw milk contains attributes that can both enhance functionality and nutritive quality of dairy products.[1] For example, raw milk contains proteins, vitamins, and beneficial fatty acids.[2] It also contains antibodies and enzymes (for example, lactoperoxidase and xanthine oxidase) that are thought to be biologically functional to improve the body's immune system but lost during thermal pasteurization.[3] Lipases and proteases in raw milk also play an important role in cheese manufacture in terms of providing unique sensory attributes to dairy products such as cheese.[4] However, all of these beneficial attributes are either lost or reduced with thermal pasteurization.[5] Yet, the number of foodborne illness outbreaks linked to raw milk is considered to outweigh any perceived or real benefits of raw milk. It is noteworthy that less than 1% of dairy products within North America are non-pasteurized yet account for over 50% of foodborne illness cases reported.[6,7] Despite the food safety risks, there remains a consumer demand for dairy products prepared from raw milk. This has necessitated the introduction of regulations to prohibit the sale or distribution of raw milk with Ontario and other parts of Canada.[8] As a compromise, there has been a sustained effort to develop non-thermal pasteurization that can ensure high quality products with extended shelf life and of course free from pathogens such as *Escherichia coli* O157:H7.[9] To date, non-thermal treatments based on pulsed electric fields.[10] supercritical carbon dioxide[11] high hydrostatic pressure[12] and high-pressure homogenization[13] have been studied in detail as an alternative to heating of milk. Although all have proven effective at reducing microbial levels, in most cases the processing technologies are expensive and/or not conducive to high capacity processing. Membrane filtration is applied commercially for non-thermal contamination of milk although a heat treatment is required to be a pasteurization process.[14] The microfiltration process has been relatively successful commercially and is used routinely for high volume production. UV decontamination has not been widely reported for milk but commonly used for pasteurization of apple juice.[15] There are several challenges in applying UV to non-thermally pasteurize milk. The most notable is the opaqueness of the matrix that restricts photon penetration thereby leading to poor decontamination efficacy. The generation of off-flavors caused by the generation of photoproducts is also a limitation along with loss of UV sensitive nutrients, such as ascorbic acid and riboflavin. It follows that if the UV exposure of milk is minimal, the generation of off-flavors and nutrient loss can be minimized but at the same time ensuring adequate reduction of microbes with complete inactivation of pathogens. Such conditions can be met through ensuring homogenous distribution of UV photons through the milk matrix thereby avoiding localized spots that lead to detrimental

production of photoproducts. To this end, the following study describes the characterization of a novel UV reactor for treating opaque fluid such as milk by ensuring efficient mixing compared to other currently available reactors.

2. MATERIAL AND METHODS

2.1 Microbes and cultivation methods

The microbes used in the study were *Bacillus subtilis* PS346 (wild type), *Bacillus* endospores, *B. subtilis* PS361 (SASP mutant; Prof P. Setlow, University of Connecticut), *Escherichia coli* K12, *E. coli* C3000, *Salmonella* Typhimurium WG49, *Lactobacillus casei*, MS2, *Salmonella* phage and T1 bacteriophages.

2.2 UV Collimated beam

The collimated beam unit consisted of a low-pressure mercury lamp (254 nm) the photons from which were directed over a Petri dish via a collimator. The Petri dish was placed on the horizontal surface below the bottom of the collimator as illustrated in. The intensity of the UV light was controlled by the distance between the end of the collimator and the Petri dish. The intensity of the UV light was measured at different points within the Petri dish area using a radiometer (Model UVX Digital Radiometer; UV Inc., Upland Canada). The sample (40 ml) to be treated was contained within a Petri dish (50 x 35mm; Kimax, Kimble Chase, Vineland, NJ, United State) placed under the collimator. Mixing was achieved via a magnetic stirrer that was set at moderate stirring rates to avoid generation of vortices. Total UV dose was calculated using the formula[16]

[IV] $E_{ave} = E_o$ x PF x WF x DF x RE

Where E_o is the measured intensity, RE is the Reflection factor, PF is the Petri dish factor, WF is the water quality factor, and DF is the divergence factor. UV dose delivered was determined for the bioassay trails by calculating the average intensity with a fixed time of UV exposure [Actual dose = E_{ave} x time = J/cm^2].

2.3 UV Taylor- Couette reactor setup

Taylor-Couette reactor was constructed in collaboration with Trojan Technologies Inc. (London, Canada). The Taylor-Couette reactor was mounted on a drill machine platform that served to rotate an inner quartz cylinder. The stationary outer cylinder was constructed from polycarbonate and sat on a stainless steel platform. The liquid to be processed was delivered

to the TC unit via a peristaltic pump (Master Flex, Thermo Fisher Scientific, Ottawa, Canada) and entered the reactor at two points of the stainless steel base. Under operational conditions the inner cylinder sat on a lubricated rubber gasket positioned below the liquid in-let. The flow rate of the liquid was modulated via the pump speed and rotation of the inner cylinder controlled by the rate of rotation of the machine head. UV was delivered via a centrally located UV lamp (0.78 W/inch; 245nm). The liquid being treated traversed the gap between the rotating and stationary cylinder then existed at the top collector plate that drained into an outlet tube. Upon completion of treatment the unit was disassembled and sanitized using a quaternary ammonium salt sanitizer (5% v/v) followed by a distilled water rinse. The surfaces were air-dried to remove residual moisture prior to the reactor being re-assembled. The inner quartz cylinder was also cleaned using iso-propanol to remove lipid residues.

2.4 Biodosimetry method

The microbe (*Bacillus* spores or bacteriophages) was suspended in test solution (distilled water, SM buffer or reconstituted skimmed milk powder-low temperature sprayed dried) and 40 ml volumes placed in a Petri dish. The Petri dish was placed under the collimated beam and samples withdrawn periodically. Spore or phage survives were enumerated as described above.

2.5 Test Liquids

The model opaque liquids tested were reconstituted skimmed milk powder (low thermal treatment spray dried milk; Gay Lee, Guelph Ontario), molasses (purchased from a local supermarket) and super Hume.

2.6 Dye tracing studies

Dye tracing studies were performed to gauge the general mixing effect within the TC reactor. Here, water was flowed through the reactor at different flow rates with the inner cylinder rotating at a defined speed. After approximately 1 liter of water had passed, 1 ml of crystal violet was introduced into the flow stream via a hypodermic needle and 10 ml fractions collected at the outlet. The absorbance at 490nm of each fraction was measured using a spectrophotometer (Biorad; Philadelphia, USA). The absorbance of each fraction was plotted again fluid volume passed to visualize the mixing effect under different reactor settings.

2.7 Visualization of different flow forms generated within a Taylor-Couette reactor

The different flow regimes generated within the TC reactor was visualized by the method described by.[17] Here, the reactor chamber (i.e. space between the cylinders) was filled with the test liquid and the inner cylinder set rotating at a defined rate. On occasions, the TC unit was held under static flow conditions where the treatment chamber was filled with fluid and crystal violet (approximately 0.1ml) injected inter the intra cylinder gap at the top collector plate. Images of the flow pattern were captured using a video camera (Sony, Tokyo, Japan) then subsequently analyzed. Different flow patterns were generated when the rotation rate of the inner cylinder and kinematic viscosity of the liquid were adjusted. With regards the latter, different kinematic viscosity liquids were produced by the addition of glycerol (Sigma-Aldrich) to the test solution (reconstituted skimmed milk or molasses). Dynamic viscosities of the fluids were tested by Brookfield DV2+ Pro Viscometer (Brookfield Engineering Labs Inc. Middleboro, MA). Studies were also performed using continuous flow to determine the effect of Reynolds number and Taylor number of fluid dynamics. The Taylor number was calculated using:

(I) $Ta = \frac{R_1 \Omega_1 d}{\upsilon}$ Where R_1 is the diameter of the inner cylinder, d is the gap between the two cylinders, υ is the kinematic viscosity of the fluid used, and Ω_1 is the velocity of the inner cylinder. Reynolds number was calculated by using[18],

(II) $Re = U_{ax} d/\nu$ where U_a means the axial velocity, d is the gap width between two concentric cylinders, and υ is the kinematic viscosity of the fluid used.

2.8 Inactivation of model microbes under different flow regimes

The test microbe was inoculated into 10 liters of the model opaque liquid at approximately 5log cfu or pfu/ml. The liquid was then passed through the UV reactor at a defined flow rate with the inner quartz cylinder rotating at a set speed. When 700 ml of the test liquid had passed through the reactor, nine samples (10 ml) were collected in sterile tubes and survivors enumerated as described above. For initial loading, samples were passed through the reactor without UV illumination prior to being enumerated. The log count reduction in microbial numbers was calculated using: Log Count Reduction = Log cfu/pfu N_i – log cfu/pfu N_o

N_i: Initial loading (control)

N_o: Surviving numbers following UV treatment

2.9 Determination of absorption coefficient

The absorbance of the samples was measured using a Cary 300 UV/V is Spectrophotometer (Varian Inc. Walnut Creek, CA) equipped with a Labsphere DRA-CA-3300 Integrating Sphere (Labsphere, North Sutton NH). Each sample was tested in triplicate before and after each UV treatment using demountable fused-quartz cuvettes (NSG Precision Cell. Inc., Farmingdale, NY) consisting of different path lengths (0.1-2 cm). The absorbance coefficient was determined from the slope of the linear plot.

2.10 UV Spectra

Ultraviolet spectra were taken to determine the change in the tryptophan absorbance as a consequence of UV irradiation. The spectrometer (Biochrom, Cambridge, United Kingdom) was operated at a resolution of 1 nm. The spectra were recorded in the wavelength region 200-400 nm. Tryptophan was irradiated at a concentration of 0.05% w/v and spectra were performed on a 1/10 dilution of tryptophan. Distilled water used for tryptophan was subtracted before absorbance readings.

2.11 Fourier Transform Infrared (FTIR) evaluation

FTIR spectra were obtained using a Fourier transform spectrometer (Shimadzu Corp., Kyoto, Japan) equipped with a total attenuated reflection accessory (Pike Technologies, Madison, Wis., U.S.A.). Spectra were scanned from 600 to 4000 cm^{-1} at 4 cm^{-1} resolutions. Prior to scanning, a measurement was taken on air as the background. IR spectra were collected at room temperature for UV treated 0.05% tryptophan at 30 averaged scans per spectrum.

2.12 Statistical analysis

The data obtained were transformed into the $\log_{10}$ prior to analyzing using ANOVA, Tukey's test (S-Plus, Insightful Crop, NY, USA).

3. RESULTS

3.1 Absorption coefficient determination for working fluids

As part of the UV dose calculations, it was necessary to determine the absorption coefficient of the skimmed milk. The traditional method of measuring the UV absorption of the liquid under test at different path lengths proved unsuccessful due to the opaque (low UV transmission) of the skimmed milk solution (Figure 3-1). Therefore, absorption coefficients used to calculate the dose were generated using the integrated sphere method (Table 3-1).

The results showed that the absorption coefficients of 0.1%, 1%, and 10% (w/v) skim milk were significantly different compared to the results obtained from the traditional method**.**

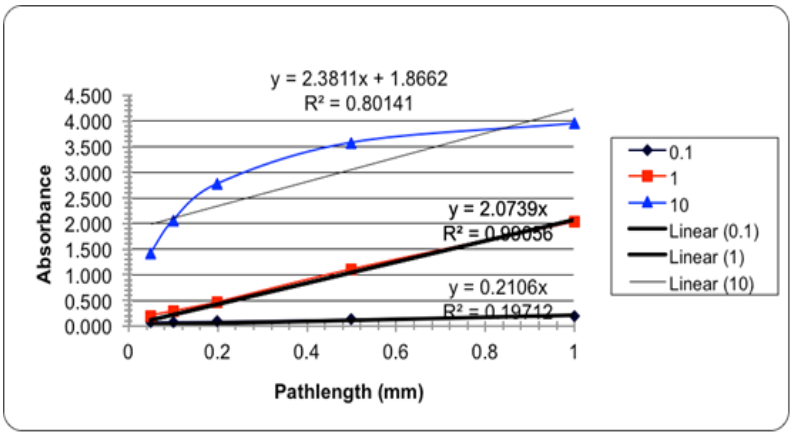

Figure 3-1: Absorbance of 1mg/ml, 10 mg/ml, and 100mg/ml skim milk tested at 254nm.

3.2. Biodosimetry using *Bacillus subtilis* endospores and bacteriophages

Trials were performed to determine the inactivation kinetics of *Bacillus* endospores and bacteriophages with the view of using the microbes as a measure of the UV dose delivered (i.e. biodosimetry) within the TC-reactor. The inactivation kinetics of *B. subtilis* PS 346 and PS 361 spores was monitored within water or skimmed milk using the collimated beam unit set at different UV intensities. The inactivation curves for the wild type *B. subtilis* spores (PS 346) suspended in water did not exhibit a shoulder and followed a logarithmic reduction (Figure 3-2). Inactivation curves of *B. subtilis* PS 346 spores suspended in skimmed milk did exhibit an initial shoulder followed by a logarithmic decrease (Figure 3-2). In terms of exposure time, it was evident that the UV inactivation of spores occurred at a slower rate in skimmed milk solution relative to water. When corrected for the higher absorption coefficient, it was also found the inactivation kinetics of PS 346 spores were significantly ($P<0.05$) slower in milk compared to water. *B. subtilis* spores suspended in 100 mg/ml (10% w/v) skimmed milk powder were significantly ($P<0.05$) more tolerant to UV compared to when 1% w/v (10 mg/ml) solutions were applied (Figure 3-3). Given that the UV dose was corrected to account for different absorption coefficients between 1% and 10% w/v skimmed milk powder solutions, it can be concluded that the milk components provide spores with a direct and/or indirect protective effect against UV photons (Table 3-2). In addition, when suspending *Bacillus subtilis* spores PS346 in 1% (w/v) skim milk, it was also evident that these endospores could germinate at room temperature (25°C). Spores (ca. 10%) suspended in skimmed milk lost phase brightness after 20 min incubation at room temperature. The

inactivation of *B. subtilis* PS 361 (SASP mutant) followed first-order inactivation with no apparent shoulder (Figure 3-4). The inactivation rate was significantly ($P<0.05$) higher in water compared to skimmed milk. This again would suggest a protective effect of the skimmed milk constituents against the lethal effects of UV photons. The rate of inactivation of PS 361 spores in skimmed milk was independent on the UV intensity with no significant differences ($P>0.05$) being observed (Table 3-2). Bacteriophages applied to measure UV dose were T1, *Salmonella* (Sal) phage and MS2 coliphage. From the inactivation curves of T1 phages in SM buffer, there was a shoulder when the applied UV intensity was 50 μW/cm^2 although less apparent at higher UV intensities (Figure 3-5). Sal phage exhibited shoulders at all UV intensities except 150 μW/cm^2 applied (Figure 3-6). In contrast, MS2 exhibited extensive shoulder at all the UV intensities applied and tailing effect only observed when 100 μW/cm^2 was applied (Figure 3-7).

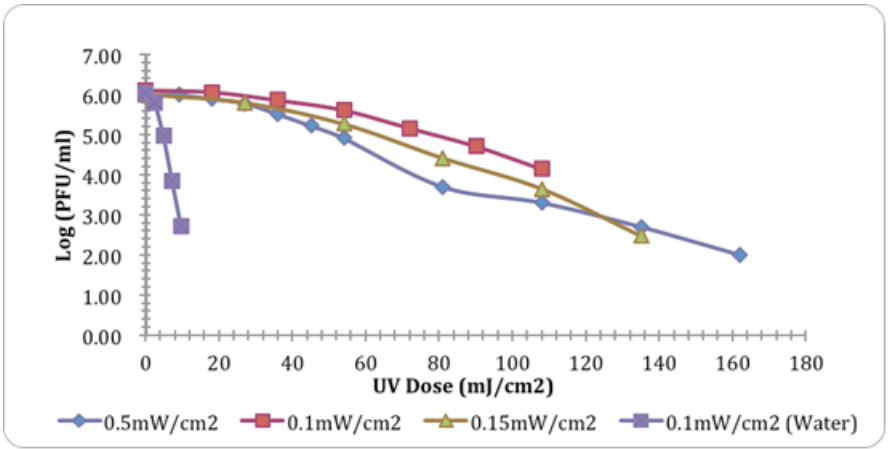

Figure 3-2: *Bacillus subtilis* spores PS346 inactivation by UV collimated beam when using 10 mg/ml skim milk or water. Different UV intensities such as 50, 100, and 150 μW/cm^2 were used.

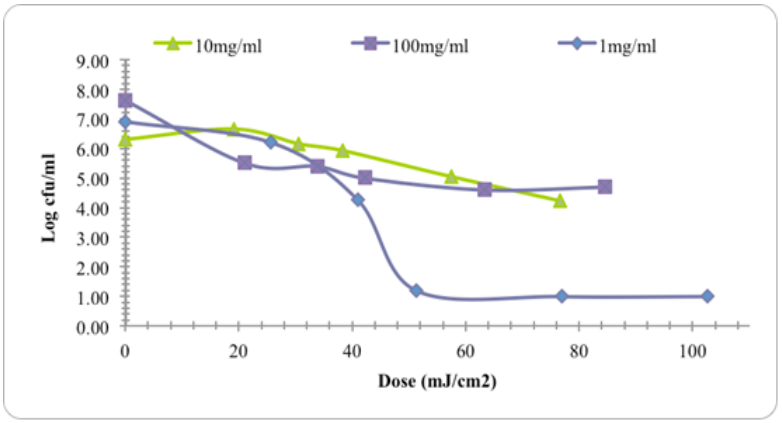

Figure 3-3: Inactivation kinetics of *Bacillus subtilis* spores PS346 in skim milk with different concentrations of skim milk such as 1mg/ml, 10mg/ml, and 100mg/ml (w/v) at 100µW/cm^2 UV intensity.

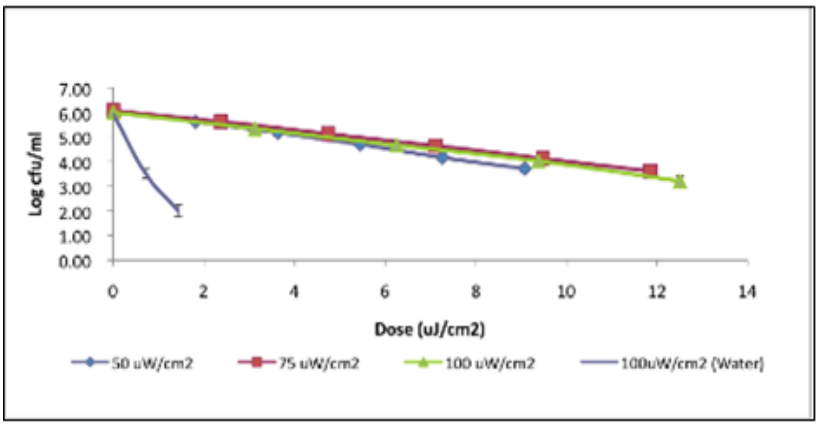

Figure 3-4: Inactivation of *Bacillus subtilis* spores PS361 (SASP mutant) in 10mg/ml skim milk or water at different UV intensities such as 50, 75 and 100µW/cm^2.

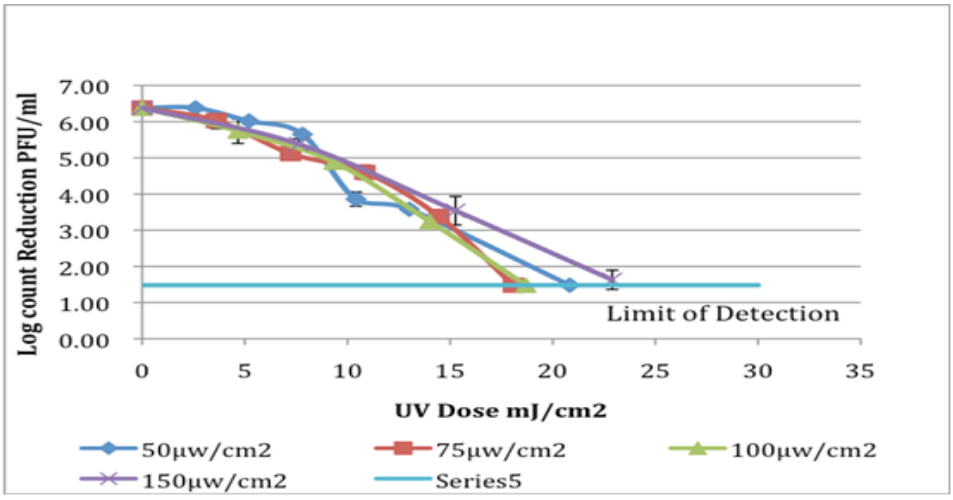

Figure 3-5: UV inactivation kinetics of T1 phages determined by collimated beam using SM Buffer at different UV intensities.

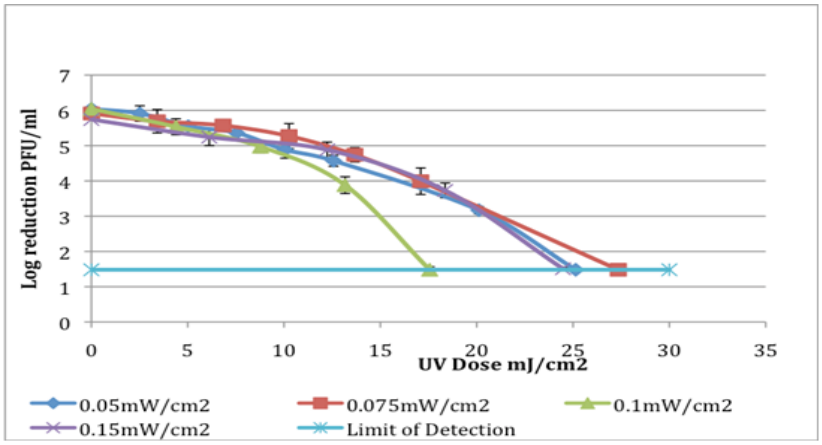

Figure 3-6: UV inactivation kinetics of *Salmonella* phages determined by collimated beam using SM Buffer at different UV intensities.

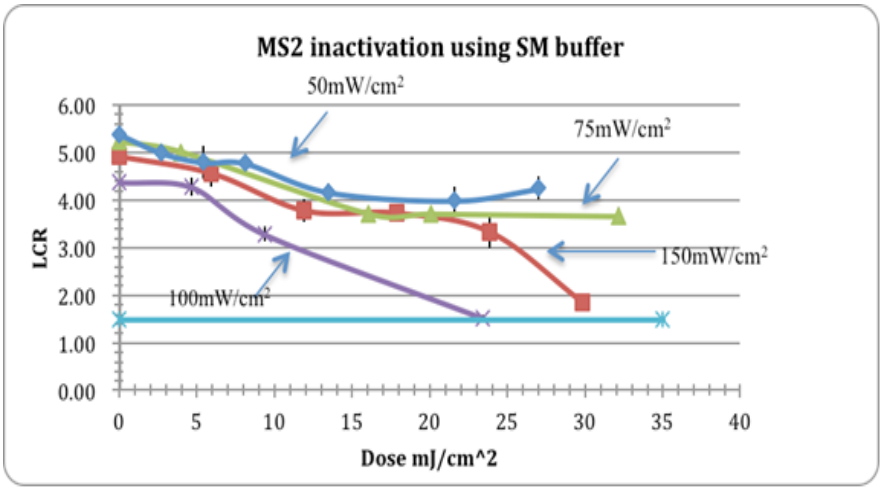

Figure 3-7: UV inactivation kinetics of MS2 coliphages determined in collimated beam UV apparatus in SM Buffer at different UV intensities.

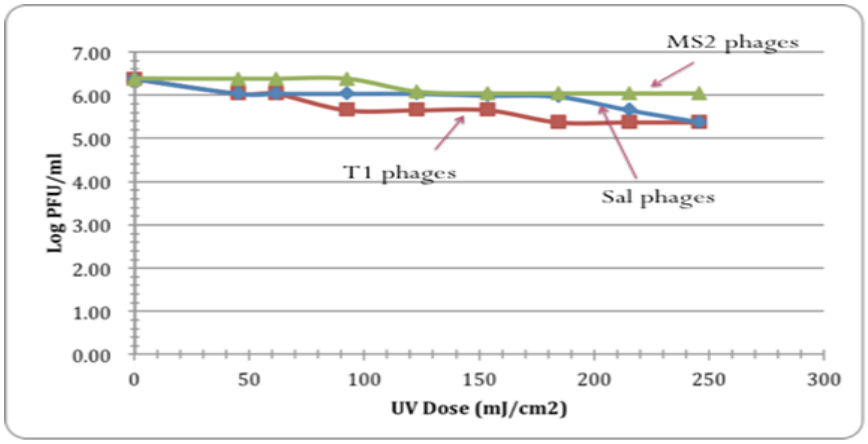

Figure 3-8: UV inactivation kinetics of bacteriophages (T1, Sal, and MS2 phages) in collimated beam UV apparatus in skim milk (10% w/v) at 50µW/cm^2 UV intensity.

Table 3-1: Absorption coefficients obtained at 254nm using integrated sphere for different solutions used in the study.

Sample	Absorption coefficient (cm^{-1})	Sample	Absorption coefficient (cm^{-1})
Molasses: glycerol (1:50)	0.63	0.1% skim milk	0.033
Skim milk: glycerol (1:50)	0.29	1% skim milk	0.3
0.1% tryptophan	0.36	10% skim milk	0.21
0.08% tryptophan	0.37	0.5% cysteine	0.02
0.05% tryptophan	0.27	1%cysteine	0.035
0.01% tryptophan	0.17	2% cysteine	0.066
SM buffer	0.014	0.5% tryptophan	0.25

Table 3-2: D_{10} values and inactivation rates of model microorganisms calculated from biodosimetry trails [using water, 1mg/ml skim milk, 10 mg/ml skim milk, or 100 mg/ml skim milk]. They were done with collimated beam at UV intensity of 0.1mW/cm^2 except for the inactivation of bacteriophages using 100mg/ml trails that was done with 0.5 mW/cm^2.

Solution	*Bacillus subtilis* spores PS346		*Bacillus subtilis* spores PS361		Sal phages		T1 phages		MS2 phages	
	D_{10}	Kill rate	D_{10}	Kill rate	D_{10}	Kill rate	D_{10}	Kill rate	D_{10}	Kill rate
Water/SM buffer	2.3	0.43	0.29	3.4	4.4	0.3	3.1	0.31	11.9	0.08
Milk 0.1%	7.6	0.1	_	_	_	_	_	_	_	_
Milk 1%	40.8	0.024	4.4	0.22	_	_	_	_	_	_
Milk 10%	52	0.015	_	_	487.45	0.002	487.45	0.002	487.45	0.002

From comparing the relative D values, it was observed that MS2 was significantly ($P<0.05$) more resistant than Sal phages that in turn were significantly ($P<0.05$) more tolerant compared to T1 (Table 3-2). The same bacteriophages were also tested using reconstituted skim milk (10% w/v). From the inactivation curves of T1, MS2, and Sal phages, it was apparent that the milk constituents provided a protective effect with only negligible log reduction in phage numbers being recorded (Figure 3-8).

3.3 Modeling and identifying different TC vortices within Taylor- Couttee reactor

3.3.1. Mathematical modeling

The different flow regimes within the Taylor-Couette (TC) reactor were modeled using a combination of different Taylor and Reynolds numbers. The objective of this part of the

study was to establish the conditions required to generate the different waveforms to identify which would support the most efficient mixing, hence microbial inactivation by UV. As described in the Introduction, the fluid flow within a TC reactor is based on the rotation of the inner cylinder, flow rate and viscosity of the liquid. To generate the different flow regimes, it was necessary to alter the viscosity of the reconstituted skimmed milk by supplementing with glycerol (Table 3-3 a and b). The Taylor number is dependent on the viscosity of the fluid and imposed centrifugal forces (Equation I; Rudolph *et al.*, 1998).

(I) $Ta = \frac{R_1 \Omega_1 d}{\upsilon}$ where R_1 is the diameter of the inner cylinder, d is the gap between the two cylinders, υ is the kinematic viscosity of the fluid used, and Ω_1 is the velocity of the inner cylinder. The predicted Taylor number was calculated from the measured liquid viscosity and rotation rate of the inner cylinder (Figure 4-9).

Reynolds number was calculated using (Giordano *et al.*, 2000, Resende *et al.*, 2001, Dumont, *et al.*, 2002, and Dusting, *et al.*, 2009),

(II) $Re = U_{ax}\, d/\nu$ where U_a means the axial velocity, d is the gap width between two concentric cylinders, and υ is the kinematic viscosity of the fluid used. Re was determined for flow rates 100, 400, 800, 1000, and 2000 ml/min for all the solutions tested (Figure 3-10).

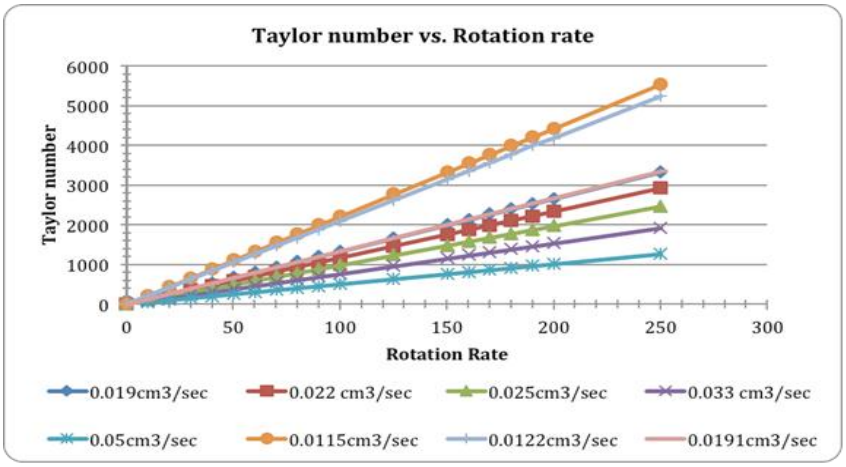

Figure 3-9: Predicted Taylor number from the measured liquid viscosity and rotation rate of the inner cylinder for skim milk solutions.

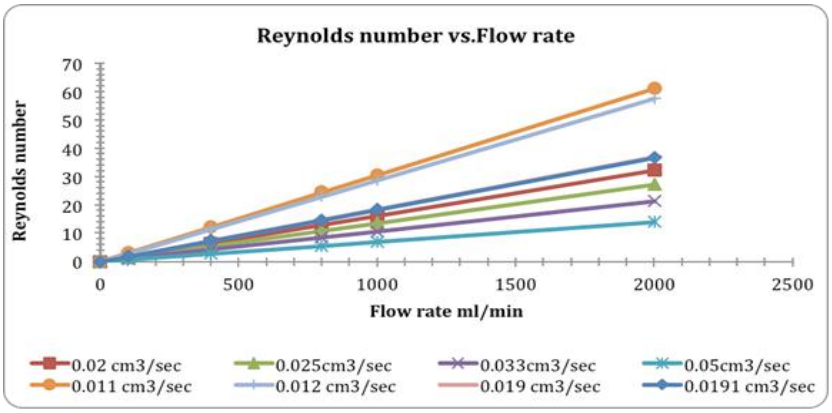

Figure 3-10: Predicted Reynolds numbers from the measured liquid viscosity and rotationrate of the inner cylinder for milk solutions.

Table 3-3: (A) Characteristics of different concentration of skim milk solutions [0.1%, 1%, and 10% (w/v)] used in the study. (B) Characteristic of 1% (w/v) skim milk supplemented with different concentrations of glycerol solutions.

A

Concentration of skim milk (g/100 ml)	Dynamic viscosity of skim milk powder (Cp)	Kinematic viscosity of skim milk powder (cm^2 /sec)	Density of skim milk powder (g/cm^3)
0.1	1.15	0.011	1.001
1.0	1.23	0.012	1.01
10	2.09	0.019	1.1

B

Concentration of glycerol (g/100 ml 1% skimmed milk solution)	Dynamic viscosity of glycerol Cp	Kinematic viscosity of glycerol and skim milk (cm^2/sec)	Density of the fluid (glycerol and skim milk) (g/cm^3)
10	2.12	0.019	1.11
20	2.64	0.022	1.21
30	3.38	0.025	1.31
40	4.66	0.033	1.41
50	7.61	0.05	1.51

3.3.2 Flow regimes using the Taylor-Couette reactor

The main function of Taylor-Couette reactor is to ensure efficient mixing thereby facilitating a homogenous distribution of UV photons. Dye tracer studies were performed to provide an initial assessment of the mixing efficiency under different reactor operating regimes. Here, the dye (crystal violet) was injected into the flow stream of water and absorbance (490 nm) monitored at the outlet.

When the reactor was held static, the dye travelled through the reactor via plug flow with a relatively narrow peak in absorbance being observed (Figure 3-11). When the inner cylinder was rotated, the absorbance of liquid at the outlet was broader indicating that the dye had been mixed (distributed). The extent of distribution was independent on the rotation rate but exhibited plug like flow with increasing flow rate (Figure 3-12). Collectively, the dye tracing studies using crystal violet confirmed that the TC-reactor induced mixing (re-distribution of dye) in the liquid and that the flow regime was more influenced by flow rate as opposed the rotation rate of the inner cylinder. To measure the biological (antimicrobial) UV dose, the crystal violet was substituted for *B. subtilis* spores. Here, spores (6 log cfu/ml) were injected into the reactor flow stream (water) and fractions collected at the outlet. It was found that a negligible reduction of spores was recovered when the inner cylinder was stationary although significantly ($P<0.05$) higher when rotating (Table 3-4). The highest reduction in spore numbers was observed at 50 rpm compared to other rotating rates were applied (Table 3-4). This would confirm that the rotation of the inner cylinder resulted in a mixing effect that increased exposure of the spores to UV (Table 3-4).

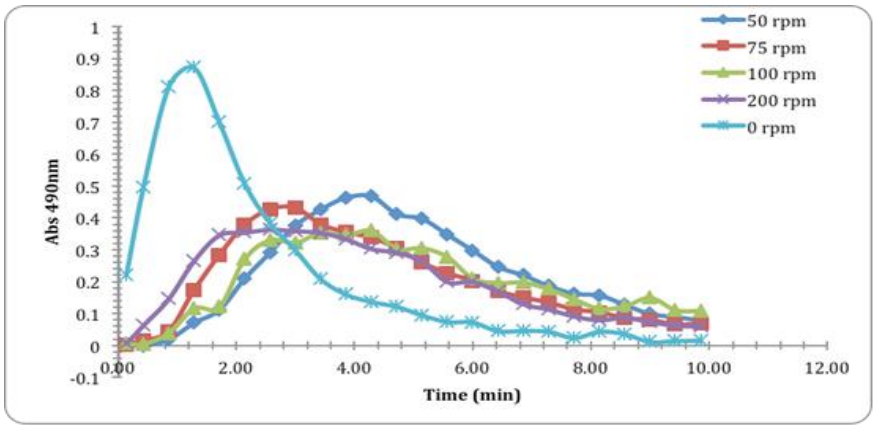

Figure 3-11: Distribution of crystal violet dye injected into the flow stream (70 ml/min) and mixed within a Taylor-Couette reactor operating at different rotation rates.

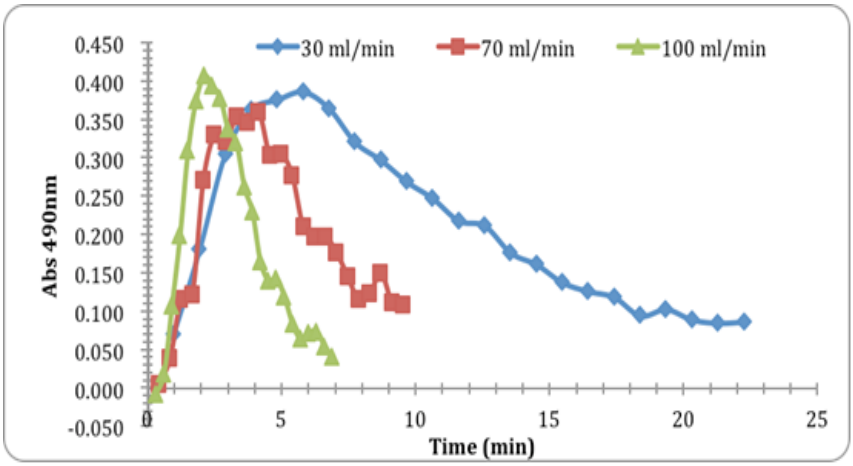

Figure 3-12: Effect of flow rate on the distribution of crystal violet introduced into the flow stream passing through a Taylor-Couette reactor operating at 100 rpm.

Table 3-4: *Bacillus subtilis* PS 346 spores suspended in water and passed through a TC reactor under different rotation rates and a flow rate of 70ml/ min.

Rotation Speed (rpm)	No UV (log cfu)			UV (log cfu)			
	F1	F 2	F 3	F 1	F 2	LCR	F 3
0	<2	6.13	3.44	<2	3.85	2.28±0.04[a]	<2
50	<3	6.00	3.51	<2	0.00	6±0.1[b]	<2
75	<3	6.09	3.64	<2	0.90	5.19±0.2[b]	<2
	3.45	6.05	0.67	<2	1.00	5.05±0.13[c]	<2

3.3.3 Visualization fluids Experiments

Although informative, the dye tracer method was insufficiently sensitive to identify the nature of vortices generated within the TC reactor. Therefore, further trials were undertaken using visualization fluids. Here, the fluids with a range of Taylor values were loaded into the reactor and rotation rate set. Dye was introduced into the top of the reactor using a hypodermic needle and syringe. Images of the flow pattern were then recorded using a video camera prior to analyzing and categorizing the flow pattern. Reconstituted skimmed milk powder (1% w/v) was supplemented with different glycerol concentrations to give kinematic viscosities ranging from 0.02 to 0.05 cm^2/sec. Different Taylor numbers were generated by altering the rotation rate of the inner cylinder. Taylor numbers ranging from 253.2 to 818.2 resulted in laminar wavy vortices (WV) whilst Ta= 934.7 - 1388.3 generated laminar modulated wavy vortices (MWV). In addition, Ta=1460-1778.3 resulted in turbulent modulated wavy vortices (TMW); however, turbulent wavy vortices were generated at Ta= 1928.4-2402.4. At higher Ta values, fully turbulent flow vortices (TV) were generated.

The transitions between these regimes were observed at different Taylor numbers (Table 3-5). When using different concentrations of reconstituted skimmed milk powder alone, Ta= 671.7 generated a laminar wavy vortices WV, while Ta= 939.6-1207.4 resulted in laminar modulated wavy vortices MWV. Also, the Ta= 1465.9-1774.3 resulted in turbulent modulated wavy vortices TMW, and Ta= 1883.8-2012.4 generated a turbulent wavy vortices TWV. In this case, the turbulent flow for skimmed milk fluids was generated at higher Taylor numbers. The transitions between these flow regimes occurred at different Taylor numbers (Table 3-6). In summary, with skimmed milk alone, the increase in rotation induced MWV, TMW and TV flow patterns. When skimmed milk was supplemented with glycerol to increase the kinematic viscosity the same vortices were observed by occurred at higher rotation rates. The effect of flow rate (Reynolds number) and rotation rate (Taylor number) on the vortex pattern was also determined. When using the 1% w/v skimmed milk mixed with glycerol, random laminar wavy vortices (RWV) waveform was observed at low rotation rates with the transition between WV and TMW occurring at higher rotation rates when Reynolds number was > 5. However, when a Re 14 was applied, the WV waveform was transient with turbulent waveforms (TWV) being generated at 180 rpm that remained until the highest rotation rate (250 rpm) tested (Table 3-7).

Table 3-5: Different flow regimes observed when using 1% (w/v) skim milk supplemented with different concentrations of glycerol under a wide range of Taylor numbers and zero Reynolds numbers.

RPM	Kinematic Viscosity of 0.019 cm^2/sec		Kinematic Viscosity of 0.022cm^2/sec		Kinematic Viscosity of 0.026 cm^2/sec		Kinematic Viscosity of 0.033 cm^2/sec		Kinematic Viscosity of 0.05 cm^2/sec	
	Ta	Flow regime	Ta	Flow regime	Ta	Flow regime	Ta	Flow regime	Ta	Flow regime
50	668.2	WV	584.9	WV	494.6	WV	386.1	WV	253.2	WV
70	934.7	MWV	818.2	WV	691.9	WV	540.1	WV	354.2	WV
80	1067.3	MWV	934.3	MWV	790	WV	616.8	WV	404.5	WV
90	1201.2	MWV	1051.5	MWV	889.2	WV	694.2	WV	455.2	WV
125	1667.9	TMW	1460	TMV	1234.6	MWV	963.9	MWV	632.1	WV
150	2002	TWV	1752.5	TMW	1481.9	TMW	1156.9	MWV	758.7	WV
180	2402.4	TWV	2103	TWV	1778.3	TMW	1388.3	MWV	910.4	MWV
200	2665	TV	2332.9	TWV	1972.7	TWV	1540.1	TMW	1010	MWV
250	3337	TV	2921.2	TV	2470.2	TWV	1928.4	TWV	1264.6	MWV

Table 3-6: Different flow regimes visualized using different concentrations of skim milk at different Taylor number and Reynolds number equal to zero.

Rotation Rates (RPM)	Kinematic Viscosity 0.011 cm^2/sec		Kinematic Viscosity 0.012 cm^2/sec.		Kinematic Viscosity 0.019cm^2/sec	
	Ta	Flow regime	Ta	Flow regime	Ta	Flow regime
50	1110.8	MWV	1047.9	MWV	671.7	WV
70	1553.86	TMW	1465.85	TMW	939.6	MWV
80	1774.32	TMW	1673.8	TMW	1072.9	MWV
90	1996.9	TWV	1883.8	TWV	1207.4	MWV
125	2772.78	TV	2615.7	TV	1676.6	TMW
150	3328.17	TV	3139.7	TV	2012.4	TWV
180	3993.8	TV	3767.6	TV	2414.9	TV
200	4430.5	TV	4179.58	TV	2678.9	TV
250	5547.67	TV	5233.5	TV	3354.4	TV

Table 3-7: Different flow regimes visualized using 1% (w/v) skim milk supplemented with 50% glycerol under a wide range of Taylor numbers (Ta) and Reynolds numbers (Re).

RPM	Ta	Re=0	Re= 0.7	Re= 2.8	Re= 5.5	Re= 7	Re= 14
50	253.2	WV	WV	WV	RWV	RWV	RWV
70	354.2	WV	WV	WV	RWV	RWV	RWV
80	404.5	WV	WV	WV	WV	RWV	RWV
90	455.2	WV	WV	WV	WV	WV	RWV
125	632.1	WV	WV	WV	WV	WV	WV
150	758.7	WV	WV	WV	WV	WV	WV
180	910.4	MWV	MWV	TWV	TWV	WV	TWV
200	1010	MWV	MWV	TWV	TWV	TWV	TWV
250	1264.6	MWV	MWV	TMV	TMV	TWV	TWV

3.3.4. Log Count Reduction of model microbes under different flow regimes

The UV inactivation kinetics of *Salmonella* phage within reconstituted skimmed milk containing glycerol was determined under the different flow patterns (Figure 3-13). The selection of Sal phages was based on their intermediate UV resistance and also to avoid error in measurements due to the induction in spore germination that would occur if *B. subtilis* spores were applied. Sal bacteriophages were inoculated into the reconstituted skimmed milk powder containing glycerol and passed through the reactor using parameters to generate the different waveforms. Samples (n = 9) were collected continuously at the reactor outlet as described in the Materials and Methods section. The log count reduction (LCR) was determined by subtracting the number of survivors recovered in the UV treated samples compared to levels passed through the reactor in the absence of UV. When the inner cylinder

was left static, there was 1.3log$_{10}$ pfu reduction that increased with the Taylor number (rotation rate). At low Ta values, the WV waveform dominated and the highest LCR of Sal phage recorded during the transition to MWV. Yet, there was a significant ($P<0.05$) lower LCR of phages in the first MWV region compared to the transition from WV and to MWV. As the Ta number increased, laminar modulated wavy vortices (MWV) were steady, resulting in a significant reduction ($P<0.05$) in LCR compared to the first region of these vortices. The Reynolds number was increased to 22.9 using 1% w/v reconstituted skim milk alone to determine the LCR of Sal phages under TWV and TV waveforms. Again, the highest LCR was observed at the transition point between WV and TWV. The LCR decreased during the transition from TRA to TV then stabilized (Figure 3-14). At mid range Reynolds number (11.6), the transition from TWV to TV was more abrupt but did not include the transitional flow (TRA). Within the TWV region, there was a decrease in LCR but increase during the transition to the TV. Yet, it was found that the highest LCR of Sal phage was observed at the transition point between TWV and TV flow but lethality progressively decreased as the Taylor number increased (Figure 3-15). In summary, from the results obtained, it was demonstrated that the extent of mixing (as evaluated from the LCR of Sal phages) occurred during the transition points between different flow patterns. The highest log reductions of Sal phage were observed during the transition between WV and MWV.

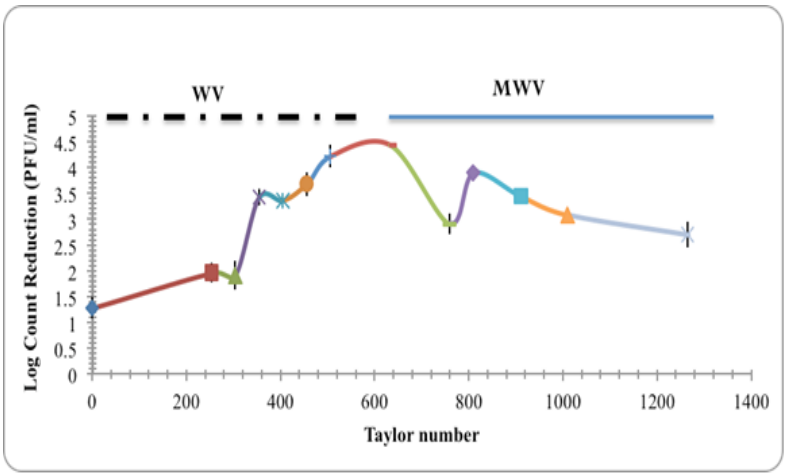

Figure 3-13: *Salmonella* phages inactivation by Taylor-Couette reactor when using 50g glycerol mixed with 1g skim milk at Re=0.7. Inactivation rate was under different flow regimes (laminar wavy vortices WV and laminar modulated wavy vortices MWV).

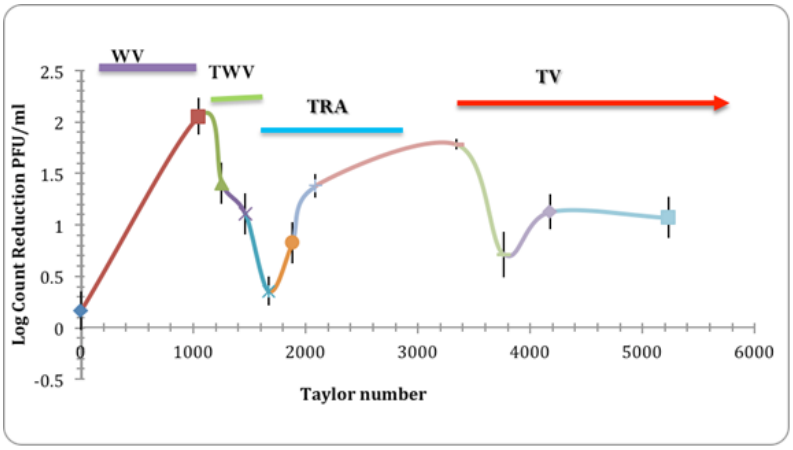

Figure 3-14: *Salmonella* phages inactivation using 1%(w/v) skim milk and tested by Taylor- Couettee reactor at Re of 22.9 under different flow regimes (laminar wavy vortices WV, turbulent wavy vortices TWV, transitional flow TRA, and turbulent vortices TV).

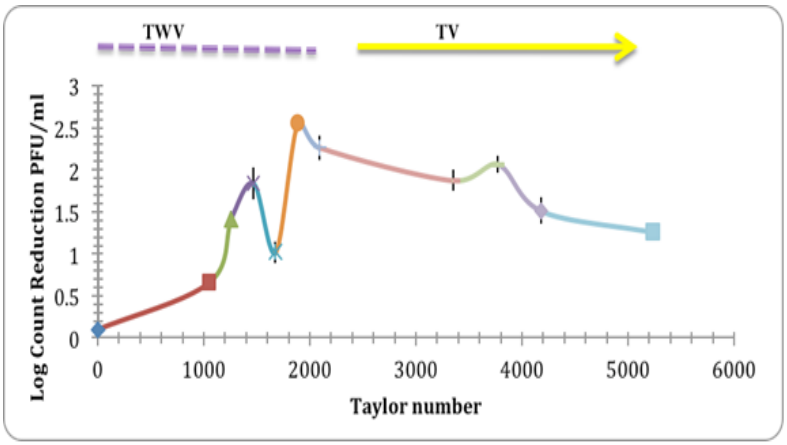

Figure 3-15: *Salmonella* phage inactivation by Taylor-Couette reactor when using 1% (w/v) skim milk solution at Reynolds number of 11.6 under two-flow regimes (turbulent wavy vortices TWV and turbulent vortices TV).

3.3.5 Determining the log reduction of microorganisms in irradiated skim milk

The solids content of fresh milk is in the order of 10% w/v solids with a kinematic viscosity of 0.019 cm^2/sec. Therefore, trials were performed to identify the predominating waveforms under comparable Ta (671.7– 3354.4) and Reynolds numbers (0 – 37). From visualization dye studies, the WV waveform observed at low Re values (0 – 1.9) with the transition to MWV and then to TMW and to TWV and to TV occurring at Ta 939.6, 1676.6, 2012.4, and 2414.9, respectively. Laminar wavy vortices (WV) were also observed at Re= 7.4 or 14.8 and were converted to TWV at Ta of 939.6 and 1072.9, respectively. At Re 18.5, the RWV waveform was generated that traversed in the WV waveform then to TWV and to TV at Ta

939.6, 1207.4, and 2012.4, respectively. At the highest Re number (Re 37) tested, the RWV flow pattern dominated with a transition to WV occurring at Ta 939.6 and to TWV at Ta 1676.6. The TRA flow regime was observed at the range of Ta of 2012.4 to 3354.4.

The LCR by UV of T1, Sal phages and MS2 bacteriophages introduced into 10% w/v skimmed milk and treated with UV using Re 1.9 (100 ml/min) was determined. The Re was selected based on the fact that this was where the transition between WV and MWV flow occurred. For T1 phages (most UV sensitive), the LCR within the WV zone was significantly ($P < 0.05$) higher compared to when the inner cylinder was stationary (Ta= 0) (Figure 3-16). A similar LCR trend was also observed for Sal phages although the level of inactivation was significantly ($P < 0.05$) lower compared to T1 bacteriophages. Only negligible, LCR of MS2 phages were observed over the range of Ta numbers tested and was significantly ($P < 0.05$) lower in the range of 1340.8-2145. The results would suggest that the MS2 phages within 10% skimmed milk under flow regimes of MWV and TMW were not exposed to sufficient UV doses to cause inactivation.

B. subtilis PS 346 spores were tested with 1% and 10% w/v skim milk under different flow regimes. Levels of *B. subtilis* PS 346 spores in 1% w/v skim milk at Re=0.075 (70 ml/min) were reduced when the imposed flow regime was laminar modulated wavy vortices (MWV), turbulent modulated wavy vortices, and turbulent wavy vortices.

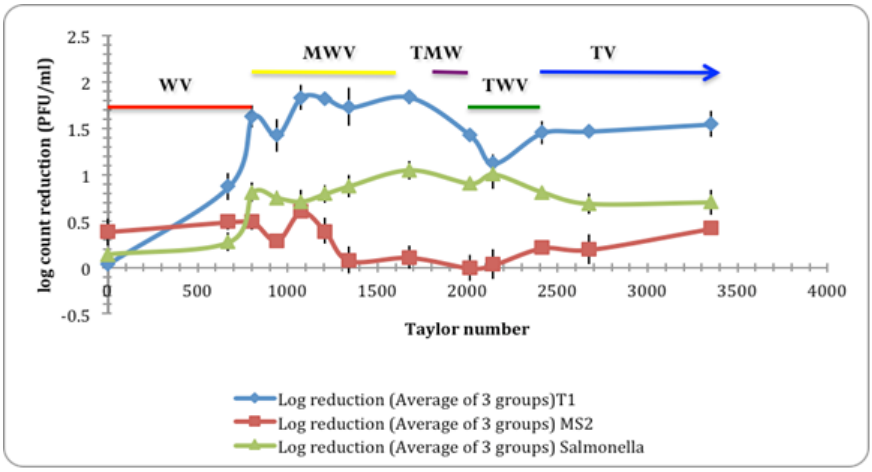

Figure 3-16: Inactivation of bacteriophages (MS2 coliphages, T1, and *Salmonella* phages) by Taylor-Couette reactor when using 10% (w/v) skim milk solution at Re=1.9 under different flow regimes (laminar wavy vortices WV, laminar modulated wavy vortices MWV, turbulent modulated wavy vortices TMW, turbulent wavy vortices TWV, and turbulent vortices TV).

However, when testing *B. subtilis* PS346 spores suspended within 10% w/v skim milk, there was insignificant (P> 0.05) log count reduction achieved regardless of the applied flow regime. This would suggest that at 10% w/v reconstituted skim milk provided spores with a protective effect against UV photons. The estimated UV doses applied in the Taylor-Couette reactor to these spores either through 1% or 10% w/v skim milk. From the results obtained, it was evident that the highest biological active UV dose was achieved with the TWV flow regime.

3.5. Inactivation of *Escherichia coli* and *Lactobacillus* in milk treated with UV using the TC-reactor: The inactivation curves of *E. coli* K12 suspended in NaCl 0.85% did not exhibit a shoulder and followed a logarithmic reduction. The tailing could be noticed at only 2 min of UV exposure. However, the inactivation kinetics of *Lactobacillus casei* (LAB) showed that there was a shoulder at lower UV doses applied followed by a logarithmic reduction. The tailing was observed at the higher UV doses applied (Figure 3-17). The D_{10} for *E. coli* K12 was 2.2 mJ/cm^2, while it was 2.8 mJ/cm^2 for LAB bacteria. The inactivation of *E. coli* K12 and *L. casei* within 10% w/v milk (introduced at 6 log cfu/ml) passed through the TC-reactor at a Ta = 1207.4 and Re=1.9 was determined. For *E. coli* K12, a 1.06 ± 0.17 log cfu was obtained with MWV flow pattern that compares to 0.09±0.04 log cfu when the inner cylinder was held stationary (plug flow). *L. casei* counts were reduced by 0.69±0.09 log cfu under MWV flow pattern that was not significantly (P>0.05) different compared to -0.03±0.08, which was achieved when the inner cylinder was kept stationary.

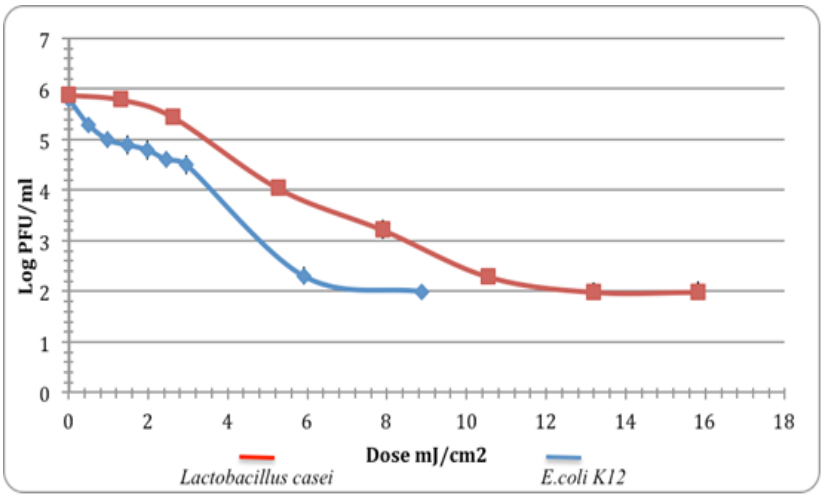

Figure 3-17: Inactivation kinetics of *E. coli* K12 and *Lactobacillus casei* when obtained from collimated beam using 0.85% NaCl.

3.6. Protective effect of milk proteins (amino acids) against UV inactivation of *Bacillus* endopsores and bacteriophages

It was evident that skimmed milk constituents provided a protective effect to microbes against UV inactivation. It is known that amino acids such as cysteine and tryptophan strongly absorb UV so could potentially enhance or negatively affect microbial inactivation. To test this hypothesis, a series of trials were performed to assess the influence of the milk matrix on the efficacy of UV treatment using the TC-reactor. Specifically, alternative matrices (super hume and molasses) with the same fluid dynamics of milk but low in protein were applied. Sal phages inoculated into super hume (30% w/v) was rapidly inactivated before UV treatment was applied. When introduced at 6-log cfu, there was 3-log cfu reduction (99.9%) before being passed through the UV reactor. The flow rate through the UV reactor was set at 100 ml/min that was the same used for 10% w/v skim milk solution, however, super hume gave a Reynolds number of 3.2. When the inner cylinder was kept stationary (Ta = 0), the LCR was 0.47±0.10 log pfu that was insignificantly ($P>0.05$) different to 0.25±0.20 log pfu when a Ta = 2086 (turbulent flow) was applied.

Molasses (30% w/v; kinematic viscosity 0.015 cm^3/sec) was inoculated with Sal phage (6 log pfu/ml) and passed through the UV reactor under turbulent wavy vortices (TWV). The LCR of Sal phages obtained under the aforementioned conditions was 0.4± 0.08 log pfu that was not significantly different ($P>0.05$) when the inner cylinder was kept stationary. To account for the different flow form of molasses compared to milk, trials were performed to increase the viscosity of the former by the addition of glycerol. When molasses was supplemented with 50% glycerol (w/v), the kinematic viscosity increased to 0.06 cm^2/sec giving an absorption coefficient of 0.63cm^{-1}. The inoculated molasses: glycerol mix was inoculated with Sal phage and flowed through the TC reactor to give a Reynolds number of 0.6 with a Ta = 373.7 (the conditions resulted in a WV flow). The LCR of Sal phage was 1.1 ± 0.2 log pfu that was insignificantly different ($P > 0.05$) compared to when the inner cylinder was held stationary (Ta = 0) that resulted in a 0.9±0.3 log pfu reduction. Collectively, the results from trials using molasses and super hume suggested that in the absence of protein, the lethality of the TC-reactor is decreased despite the mixing effect. To further test the effects of UV on proteins, trials were performed to determine the effect of the inclusion of ultraviolet absorbing amino acids (cysteine and tryptophan) on the inactivation kinetics of Sal phage.

The UV inactivation of Sal phage in a range of cysteine solutions was determined (Figure 4-18). It was noted that increasing concentrations of cysteine significantly ($P < 0.05$) decreased the UV inactivation rates of Sal phage (Figure 3-18). The effect was most notable at 2% w/v but also occurred at lower concentrations 0.5 - 1.0% w/v. A similar effect was observed when cysteine was substituted with tryptophan (Figure 4-19). Here, an extensive shoulder was observed in Sal phage inactivation when suspended in 0.08% w/v tryptophan with lower UV inactivation rates at lower concentrations of the aromatic amino acid (Figure 3-19). FT-IR spectroscopy was undertaken to determine if UV exposure resulted in changes to the structure of tryptophan. The spectra collected of tryptophan that had not been exposed to UV showed a typical banding pattern. The distinctive bands at 1579 cm^{-1}, 1620 cm^{-1} and 3398cm^{-1} correspond to carboxylic group, COO^- vibration, NH_2 vibrations, respectively. The infrared spectra of UV exposed tryptophan varied in intensity although no additional peaks were observed indicating that no structural changes to the 2,3-bond of the indole ring in tryptophan had occurred by exposure to ultraviolet light (Figure 3-20). However, differences were observed when UV spectra of tryptophan were measured (Figure 3-21). The absorption peak centered around 275nm progressively decreased with exposure time to UV at 254 nm. The results suggested that some alternation in the conjugation of tryptophan occurred due to UV exposure although this did not result in degradation reactions.

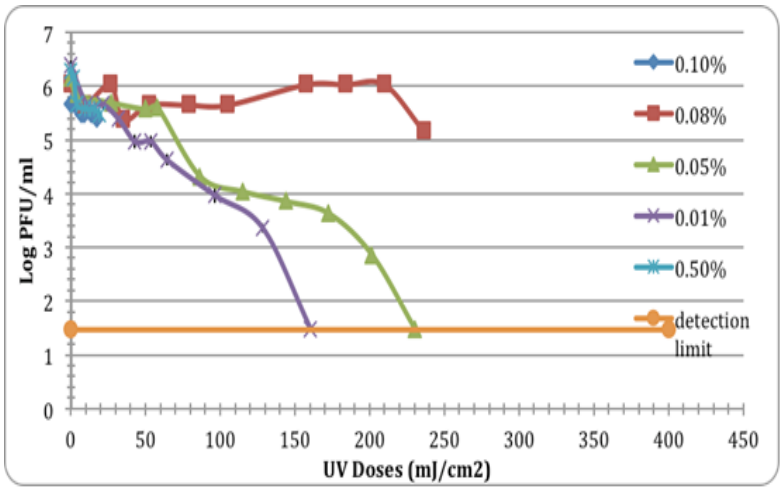

Figure 3-19: Inactivation kinetics of *Salmonella* phages obtained from collimated beam studies when using different concentrations of tryptophan at 50µW/cm^2.

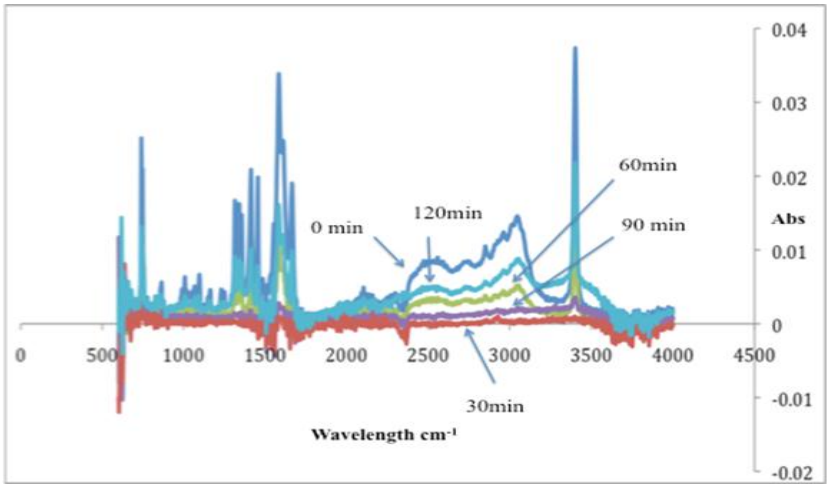

Figure 3-20: FT-IR of UV treated 0.05% w/v L-tryptophan.

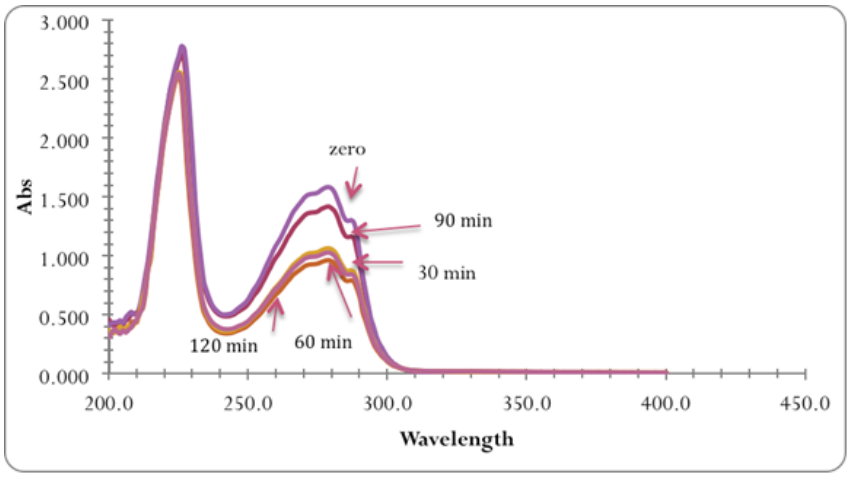

Figure 3-21: UV spectra of treated tryptophan (0.05%) at 200-400nm.

4.1. DISCUSSION

The D_{10} for the different microbes used for biodosimetry was determined using collimated beam. It was demonstrated that MS2 phages were more resistant to UV irradiation than T1 and Sal phages (Table 3-2). The D_{10} value of 11.2 mJ/cm^2 obtained in the current study compares with 20 mJ/cm^2 reported by Chevrefils[19] 18 mJ/cm^2 by other researchers[20] and 16 mJ/cm^2 by[21] Hijnen *et al.,* (2006). The underlying reasons for the diverse range of D values for MS2 UV inactivation could be attributed to a number of factors. For example, the method used to enumerate survivors would have an effect on the observed inactivation kinetics. In the majority of studies undertaken to date, the agar overlay method is applied where aliquots of test suspension is spotted onto a cell lawn of the host cell and number of plaques enumerated.[22] With specific reference to MS2, the plaques have a tendency to be diffuse and

ill defined that makes accurate enumeration problematic.[23] In the current study a MPN based method was applied that provides a more reliable approach for enumerating phages.[22]

The D_{10} value for T1 phages ranged from 3.2 – 5.1 mJ/cm^2 that is in agreement with that reported for the bacteriophage by others[24] (Abrahamian, 2010). The higher UV resistance of MS2 phage can be attributed to the more stable RNA compared to T1 that is a DNA phage.[21]

The D_{10} for *Bacillus subtilis* PS346 spores in water was 2.3 mJ/cm^2 that was significantly higher compared to the SASP mutant (PS 361). The higher UV resistance of PS346 spores compared to the mutant type (PS 361) spores is in agreement with others.[25] In the absence of SASP, the photoproducts generated within the DNA during the UV illumination differ from the spore photoproduct that cannot be readily repaired during germination.[26] There in the absence of SASP the resistance of spores is comparable to that of vegetative cells.[26]

For all the microbes tested, it was evident that the milk matrix was protective against the lethal effects of UV with higher D_{10} values being recorded compared to when measured in water or SM buffer. In the case of *Bacillus* spores, it was noteworthy that the apparent UV resistance increased in milk despite the fact that germination was induced during the exposure period. Upon spore germination, the protective SASP proteins are degraded thereby reducing the observed UV resistance[27] (Setlow, 2003). In the current study, it is likely that germination was induced in a small proportion of spores given that the PS 346 wild type was more resistance to UV than PS 361 when treatment was performed in milk. The increase UV resistance of bacteria and phages in milk compared to water is in agreement with others although the underlying mechanisms remain unclear.[28] Yet, from the results obtained, there was strong evidence to suggest a role of cysteine and tryptophan that effectively absorb UV photons. It was noteworthy in the current study that the inactivation rates of both spores and phages in solutions of cysteine and tryptophan were comparable to studies performed in skimmed milk. This would provide supporting evidence that the absorption of UV photons by tryptophan and cysteine, amongst others, was responsible for the protective effect.[30] However, it is known that the interaction of UV with cysteine and tryptophan can generate antimicrobial photoproducts. For example, UV degradation of tryptophan results in the formation of *N*- formylkynurenine.[31] In the current study, no evidence from the FTIR spectra was obtained to suggest *N*- formylkynurenine formation. Yet, it was clear from the UV spectra that a differential shift of the indole ring had occurred but without any photo-

degradation reactions that known to be performed after 24hr of UV exposure such as *N*-formylkynurenine.[31]

Although milk proteins provided UV protection, it was interesting to note that the level of Sal phage inactivation was lower in molasses used as the suspending medium. This may suggest that the UV photon scattering by milk constituents (for example, micelles) contributes to the overall inactivation kinetics although this is likely to be relatively minor compared to absorption events.[32]

Given the poor UV penetration into the milk matrix, it was likely that photons would only penetrate at μm depths at the quartz: solution interface. This finding is supported by the effect of flow-form on the level of inactivation achieved using the UV Taylor-Couette reactor. By modulating the flow rate, cylinder rotation, and viscosity of the skimmed milk, it was possible to generate a broad spectrum of fluid flow-forms. The transition from laminar (plug flow), through laminar vortices, wavy vortices and finally turbulent flow were observed through dye tracing studies. From dye distribution studies, it was evident that under moderate rotation rates, the crystal violet became dispersed within the reactor. Such a distribution is conformation of back mixing (commonly referred to as macromixing). Richter *et al.*[33] described Taylor-Couttee flow in terms of macromixing and micromixing effects. Macromixing describes the displacement of particles along the axis with micromixing being related to circulation of fluid within Taylor-Couttee vortices. From an operational standpoint (for example, in a chemical reactor), the main aim is to minimize macromixing (back-mixing) in order to decrease dispersion of reactants in a heterogenous, uncontrolled manner.[33] In contrast, micromixing (i.e, mixing within the vortex) should be maximized given the residence time of reactants within the reactor is reduced, homogenous and more defined with minimal dispersion. In the current study, it was evident that macromixing effect increased with decreasing flow rate (low Re) and less prominent at high Re values (Figure 3-11 and 3-12). However, as identified in the current study, increasing the flow rate, coupled with low viscosity, has an adverse effect on the stability of the Taylor-Couette vortices thereby narrowing the Ta range where vortices are generated.

In the current study, it was noteworthy that the highest log reductions of Sal phage were observed at the transition point between laminar wavy and modulated wavy vortices. From the many theoretical studies performed on Taylor-Couette vortices, it has been proposed that the transition between laminar to wavy vortices provides optimal micromixing.[33] Here, the

vortices move through the reactor as discrete bands (vortices) with negligible macromixing. As the Ta increases, the vortices become increasingly wavy then to turbulent along the axial-flow. With high viscosity fluids, the same effects are observed but at higher rotation rates due to the broadening and displacement of the critical Ta value to higher levels.[33] It was for this reason that the highest log reduction was achieved using skimmed milk supplemented with glycerol to increase the fluid viscosity, hence stability of the vortices generated.

In contrast, in 1% w/v skimmed milk without glycerol, the same optimal level of Sal phage inactivation was observed at the transition point from Laminar Wavy vortices and Turbulent Wavy Vortices although decreased within the Turbulent Wavy Vortices (TWV). However, the log reduction of Sal phages increases as the flow-form became increasingly turbulent (Fig 3-14). The results clearly indicate that with low viscosity liquids at least, the working parameters of the UV-Taylor Couette reactor need to be carefully selected to achieve optimal antimicrobial efficacy. Yet, it was noted that turbulent vortices provided sufficient mixing to expose phages to the UV although the levels of inactivation were significantly lower compared to the transition point between laminar vortices and TWV. Yet, it is noteworthy that in such turbulent zones, the LCR was consistent over a broader Ta range. In this respect, reactors based on turbulent flow maybe of more practical value compared to Taylor-Couette based reactors.

Trials performed in 10% v/v skimmed milk exhibited different phage inactivation profiles when UV treated under the range of flow-regimes. Here, there was an increase in LCR of T1 and Sal phage at the transition point between Laminar Wavy Vortices and Modulated Wavy Vortices. However, the LCR for Sal phage were consistent over the different Ta numbers. The LCR reduction of T1 phages decreased under turbulent flow as MS2 phage inactivation did (Figure 3-16). The different LCR obtained in 10% w/v skimmed milk compared to 1% concentration could not be explained by the former having a higher absorption coefficient, as both were comparable. However, the viscosity of 10% skimmed milk was greater compared to 1% solutions that may have facilitated stabilization of the vortices.[17]

It was noted that the LCR of Sal phages by UV in 10% w/v skimmed milk was significantly ($P < 0.05$) lower compared to when 1% w/v was used as the suspension medium. This may have been unexpected given that the vortices appeared to be stable over a wider range of Taylor numbers. It is likely that the decreased efficacy of UV to treat phages in 10% w/v was related to the higher protein (UV absorbing amino acids) content. This was supported by the

collimated beam studies where the log reduction of all phage types was negligible when suspended in 10% w/v skimmed milk.

An additional factor to explain the different LCR reductions obtained when 1% skimmed milk acted as the carrier could be related to the actual exposure time of phages to UV. It was noteworthy that the log reduction of MS2 phages (most UV resistant) was low and decreased further under Modulated Wavy Vortices. This would suggest that the phages were not being exposed to UV either through inefficient mixing or only being exposed to ultraviolet for a brief period. In contrast, T1 phage (UV sensitive) numbers decreased significantly under the same conditions. On the assumption that exposure time for both T1 and MS2 was the same, it can be concluded that the vortices travelled at a greater velocity (by virtue of vortex stability) in 10% w/v skimmed milk compared to 1% w/v skimmed milk. Therefore, although exposed to the same levels of UV, the higher sensitivity of T1 phages resulted in a greater log reduction. This hypothesis was further supported by the inactivation curves obtained from collimated beam studies. Here, MS2 exhibited extensive shoulders illustrative of a greater number of photon strikes required to inactivate the phage.[21] In contrast, T1 phage inactivation curves did not exhibit shoulders illustrative that only a small number of photon strikes lead to inactivation.

By using the level of phage inactivation, it was possible to estimate the UV dose delivered within the Taylor-Couette reactor. Within 10% w/v skimmed milk, the lowest dose was under plug flow supporting the finding that without mixing the UV is restricted. However, the generation of vortices increased the measured UV dose delivered reflective of the microbes being brought from the liquid bulk to the quartz: UV interface. The delivered UV dose was higher for high viscosity (i.e. skimmed milk supplemented with glycerol) by virtue of more stable Taylor-Couette vortices being generated. Yet, the relatively low log reductions achieved when 10% w/v skimmed milk as the carrier solution underlined the limitation of the reactor for non-thermal pasteurization of milk. Such a conclusion is supported by only 1log cfu reductions of *E. coli* K12 and *Lactobacillus* in 10% w/v skimmed milk treated under the optimized reactor operating conditions.

In comparison to other UV reactor formats, the Taylor Couette appeared to be relatively ineffective approach for decontaminating milk. Matak *et al*.,[5] described a UV reactor based on flowing milk (similar to the Cidersure) over UV tubes and reported a >5 log reduction of *Listeria monocytogenes* for the equivalent dose required by the Taylor-Couettee reactor to

decrease Sal phages counts by 3 log cfu. The Pure UV Reactor described by Reinemann *et al.*,[33] required 0.5 kJ/l (500 mJ/cm^2) to achieve a 1log reduction of *E. coli*, while Taylor-Couette reactor used in the current study required 2.3 mJ/cm^2 to reduce 1log cfu of *E. coli* initial population. In this respect the Taylor Couettee reactor can be considered to be more effective than the Pure UV reactor.

A Shockwave Power Reactor (SPR) that was based on Taylor –Couette mixing achieved a 3 log cfu reduction of *E. coli* in skimmed milk by applying an estimated 700 J/m^2[28] The SPR reactor had larger dimensions compared to the Taylor-Couettee used in the current study hence comparisons between the two may not be appropriate. It was also noted that Milly *et al.*[28] used chemical actinometry to measure the UV dose that might have provided an over-estimation of the antimicrobial UV dose applied. Yet, it was noteworthy that the optimal inactivation of *E. coli* in the SPR reactor was achieved using Ta 1800 that should in theory generate MWV; the waveform that supported the highest extent of microbial inactivation in the current study.

CONCLUSION

Biodosimetry trails were first done in attempts to calculate the D_{10} value of the model microorganisms and use these values to estimated UV doses applied to the fluids within Taylor-Couette reactor. Fluid dynamics studies showed that there were different flow regimes performed within Taylor- Couette reactor such as laminar wavy vortices WV, laminar modulated wavy vortices MWV, random laminar wavy vortices RWV, turbulent modulated wavy vortices TMW, turbulent wavy vortices TWV, transitional flow TRA, and turbulent flow TV. The highest log count reduction was achieved at the transition from WV to MWV although acceptable log count reduction was achieved at the transition between WV to TWV. Turbulent flow provided low LCR at high Reynolds numbers. When using 10% skim milk, it was shown that skim milk components, especially tryptophan, affected on the inactivation level of microorganisms. It is shown in the study that the UV spectra of tryptophan indicated some changes in the tryptophan environment although the FT-IR analysis did not show any red shifts in the tryptophan structure.

ACKNOWLEDGMENT

Special thanks to Prof. Keith Warriner for his great support and impression that breaths more than a supervisor and for giving me the guidance that helped me to materialize this project.

REFERENCE

1. Dhiman T. R., Nam S.H. Ure A.L. 2005. Factors affecting conjugated linoleic acid content in milk and meat. Critical Reviews in Food Science and Nutrition, 2005; 45(6): 463-482.
2. Henning D.R., Baer R.J., Hassan A.N., and Dave R. Major advances in concentrated and dry milk products, cheese, and milk fat-based spreads. Journal of Dairy Science, 2006; 89(4): 1179-1188
3. Silanikovea N., Shapiroa F., Shamaya A., Leitnerb G. Role of xanthine oxidase, lactoperoxidase, and NO in the innate immune system of mammary secretion during active involution in dairy cows: manipulation with casein hydrolyzates Free Radical Biology & Medicine, 2005; 38: 1139–115.
4. Cogan T.M., A review of heat resistant lipases and proteinases and the quality of dairy products. Ir. J. Fd Sci. Technol., 1977; 1: 95-105.
5. Matak K., Sumner S.S., Duncan S.E., Hovingh E., Worobo R.W., Hackney C.R., and Pierson M.D. Efficacy of UV light for the reduction of Listeria monocytogenes in Goat's milk. Journal of Food Protection., 2005; 68(10): 2212-2216.
6. Granzow L., Illnesses associated with unpasteurized dairy products. Amonthly publication of the epidemiology resources center., 2007; 10(4): 1-15.
7. Bradley, Pickering, and Jareb Advice families against giving children unpasteurized milk. 29 (12) 1-2. Retrieved from www.aapnews.org. 2008.
8. Anon. Got raw milk? Do not share Ontario dairy board warns farmer. Retrieved from www.cbc.com. 2007.
9. Matak K., Sumner S.S., Duncan S.E., Hovingh E., Worobo R.W., Hackney C.R., and Pierson M.D. Effects of UV irradiation on the reduction of bacterial pathogens and chemical indicators of milk. Retrieved from http://scholar.lib.vt.edu/theses/available/etd-12012004-170927/unrestricted/ETD1.pdf. 2004.
10. Fernandez M., Manzano S., Hoz L., Ordonez J.A., and Hierro E. Short communication: Pulsed Light Inactivation of *Listeria monocytogenes* Through Different Plastic Films. Foodborn pathogens and disease., 2009; 6(10): 1265-1267.
11. Yuk H.G., Geveke D.J., Zhang H.Q. Efficacy of supercritical carbon dioxide for non-thermal inactivation of Escherichia coli K12 in apple cider. Int. J. Food Microbial., 2009; 31(1-2): 91-99.
12. Mert M. Effect of high hydrostatic pressure on microbial load and quality parameters of grape juice. Retrieved from http://etd.lib.metu.edu.tr/upload/12611536/index.pdf. 2010.

13. Arroyo G., Sanaz P.D., Prestamo G. Effect of high pressure on the reduction of microbial populations in vegetables. Journal of Applied Microbiology., 2003; 82(6): 735-742.
14. Greaves P.L., Grosvenor R.I., and Martin B.W. Factor affecting the stability of viscous axial flow in annuli with a rotating inner cylinder. Int. J. Heat & Fluid Flow., 1983; 4(4): 187-197.
15. Koutchma T., UV light for processing foods. Journal of Science and Engineering., 2008; 30: 93-98.
16. Bolton J. R., Linden K. G., Standardization of methods for fluence (UV dose) determination in bench-scale UV experiments. Journal of environmental engineering., 2003; 209-215.
17. Ohmura N., Kataoka K., Shibata Y., and Makino T. Effective mass diffusion over cell boundaries in a Taylor-Couette flow system. Chemical Engineering Science., 1997; 52(11): 1757-1765.
18. Dusting J., Imomoh E., and Balabani S. Stability and temporally- resolved measurement of laminar mixing induced by Taylor vortex motion. European Conference on mixing. 2009; 1- 8.
19. Chevrefils G., Caron E., Wright H., Sakamoto G., Payment P., Barbeau B., and Cairns B. UV dose required to achieve incremental log inactivation of bacteria, protozoa, and viruses. IUVA News. 1999; 8(1): 38-45.
20. Koutchma T., Forney L.J., and Moraro C.I. Ultraviolet light in food technology principles and applications. 2009; ID. -13: 978-1-4200-5950-2.
21. Hijnen W.A.M., Beerendonk E.F., and Medema G.J. Inactivation credit of UV radiation for viruses, bacteria and protozoan (oo) cysts in water: a review. Water Research, 2006; 40: 3-22.
22. Hoff J.C. and Jakubowski W. Application of an end point dilution method to bacteriophage assay. Applied microbiology., 1966; 14(3): 468-469.
23. Kylberg J., Bendig M., and Drexler H. Characterization of transduction by bacteriophage T1: time of production and density of transducting particles. Journal of virology. 1975; 16(4): 854-858.
24. Abrahamian R., Wastewater Ultraviolet disinfection 1. Retrieved from http://www.iwawaterwiki.org/xwiki/bin/view/Articles/WastewaterDisinfection_0 2010.
25. Warriner K., Rysstad G., Murden A., Rumsby P., Thomas D., Waites W.M. Inactivation of Bacillus subtilis spores on aluminum and polythelene preformed cartons by UV-excimer laser irradiation. JOURNAL OF FOOD PROTECTION, 2001; 63(6): 753-757.

26. Setlow B., Melly E., and Setlow P. Properties of Spores of Bacillus subtilis Blocked at an Intermediate Stage in Spore Germination. JOURNAL OF BACTERIOLOGY. 183(16): 4894–4899.
27. Setlow B., Cowen A.E., and Setlow P. Germination of spores of *Bacillus subtilis* with dodecylamine. Journal of Applied Microbiology. 2003; 95: 637-648.
28. Milly P.J., Toledo R.T., Chen J., and Kazem B. Hydrodynamic cavitation to improve bulk fluid to surface mass transfer in a nonimmersed ultraviolet system for minimal processing of opaque and transparent fluid foods. Journal of Food Science 2007; 72(9): M407- M412.
29. Forney L.J., Pierson J.A., and Ye Z., Juice irradiation with Taylor-Couette flow: UV inactivation of *Escherichia coli.* [Abstract]. Journal of Food Protection., 2004; 67(11): 2410-2415.
30. Kehoe J., Remondetto E., Subirade M., Morris R., Brodkorb A. Tryptophan-mediated denaturation of *β*-lactoglobulin A by UV irradiation. J. Agric. Food Chem., 2008; (56): 4720-4725.
31. Chen P., Carroll T., Pearce L.E., Fletcher A.J.H. Ultraviolet inactivation of bacteria in cheese whey., 2001.
32. Richter O., Hoffmann H., Kraushaar-Czarnetzki B. Effect of the rotor shape on the mixing characteristics of a continuous flow Taylor-vortex reactor. Chemical Engineering Science, 2008; 63(13): 3504-3513.
33. Reinemann D.J., Gouws P., Cilliers T., Houck K., and Bishop J.R. New methods for UV treatment of milk for improved food safety and product quality. 2006 ASABE Annual International Meeting., 2006; 1-9.